FUDMA Journal of Sciences (FJS)
ISSN online: 2616-1370
ISSN print: 2645 - 2944
Vol. 8 No. 6, December, (Special Issue) 2024, pp 455 - 460
DOI: https://doi.org/10.33003/fjs-2024-0806-2965

PRODUCTION AND CHARACTERIZATION OF ANTI-DIABETIC GOLD NANOPARTICLES USING THE LEAF EXTRACT OF *MANGIFERA INDICA*

***[1]Badeggi, U. M., [2]Muhammad, B. L, [3]Shaba, F. A., [1]Muhammad, A. M., [1]Muhammad-Idris, H. L, [4]Sulaiman, S. R., [1]Azeh, Y. and [1]Musah, M.**

[1]Department of Chemistry, Faculty of Natural Sciences, Ibrahim Badamasi Babangida University, Niger State, Nigeria
[2]Department of Physics, Faculty of Natural Sciences, Ibrahim Badamasi Babangida University, Niger State, Nigeria
[3]Microbiology Unit, School of Prelimnary Studies, Agaie, Ibrahim Badamasi Babangida University, Niger State, Nigeria
[4]Department of Biochemistry, Faculty of Natural Sciences, Ibrahim Badamasi Babangida University, PMB 11, Lapai, Niger State, Nigeria

*Corresponding authors' email: umbadeggi@ibbu.edu.ng

ABSTRACT

Diabetes has continued to affect the well-being of millions of individuals all over the world. More than seventy percent of Africans have undiagnosed diabetes mellitus, with Nigeria among the list of the African countries recording most undiagnosed cases. Biologically synthesized gold nanoparticles using the extracts of plants have continued to gain grounds in the treatment of diabetes. In the present research, a straightforward green method was used to form gold nanoparticles (AuNPs) from *Mangifera indica* leaf extract. Transmission electron microscopy (TEM), dynamic light scattering (DLS), ultraviolet visible spectroscopy (UV-Vis), X-ray diffraction (XRD), and selected area electron diffraction (SAED) were used to characterize the nanoparticles. Using XRD and SAED, the AuNPs' crystallinity was ascertained. The TEM revealed particles of various morphologies, and the UV-Vis revealed a surface plasmon resonance (SPR) at 539 nm. The stability of the colloidal suspension was implied by the DLS measurement, which revealed a hydrodynamic size of 31.74 nm and a zeta potential of -23.7 mV. With percentage inhibitions that were about equivalent to that of acarbose, the conventional medication, the AuNPs demonstrated strong antidiabetic efficacy against the alpha-glucosidase and alpha-amylase enzymes. The research revealed the potential of *Mangifera indica* leaf extract-mediated gold nanoparticles in treatment of diabetes.

Keywords: Green nanotechnology, *Mangifera indica* extract, Green synthesis, Enzymes

INTRODUCTION

The production of gold nanoparticles has been the focus of recent research efforts due to its many potential applications (Ashraf et al., 2019). Both physical and chemical approaches have been used to manufacture them, but they require a lot of energy and complex equipment (Maddinedi et al., 2017). Additionally, they limit their applicability in some disciplines, such as biomedicals, and involve the use of strong chemicals that are harmful to the environment (Lee et al., 2014). The green synthesis techniques are a superior substitute to lessen these disadvantages.

Microorganisms and plants are examples of natural items that are utilized as precursors in the green synthesis of nanomaterials. At low temperatures, environmentally friendly reagents like water are frequently used. Because the procedure is eco-friendly, the final product is suitable for several biological applications. Gold nanoparticles using plant have been synthesized severally (Ashraf et al., 2019). This is as a result of the ease in its synthesis, the safety of the environment as harsh chemicals are not involved, the biocompatibility of the as-synthesized gold nanoparticles and applications in many biological assays. Consequently, several recent research works have demonstrated the effectiveness of gold nanoparticles in the treatment of diabetes (Badeggi et al., 2020; Ponnanikajamideen & Rajeshkumar, 2019).

The outbreak of deadly diseases all over the world, including the recent Coronavirus (Covid-19), has warranted an increased search for remedies. Although it is a disease that has been with us for a long time, diabetes has continued to affect the well-being of millions of individuals all over the world, especially those with other health challenges. More than 70% of Africans have undiagnosed diabetes mellitus, according to the International Diabetes Foundation (IDF) (Cho et al., 2018; Renner et al., 2020). Of these, it was said that 50% lived in South Africa, Nigeria, Ethiopia, and the Democratic Republic of the Congo. In 2017, there were 425 million people aged 20 to 79 who were affected by diabetes. This figure represents roughly 10% of the global population. Without adequate management, this condition is estimated to have increased by 48% in 28 years (Cho et al., 2018). Consequently, there is a greater need for substitutes that might be less expensive, safer, and more efficient. Green nanotechnology could offer this substitute.

Mangifera indica L. (Mango) belongs to the family *Anacardiaceae*. Mango is probably the most popular fruit of the tropics, a national tree to the people of Bangladesh, and a nationwide fruit of the Philippines and Indians. Mango is native to India and Southeast Asia since it has been cultivated in these regions for more than 4000 years for its good quality fruit. At present, Mango is also grown in Central America, Europe, Australia, and Africa. Although over a thousand mango fruits exist worldwide, only a handful is produced on a large scale (Olotu et al., 2020). In Nigeria: Kogi, Yobe, Kaduna, Sokoto, Adamawa, Plateau, Benue, and Niger states are the main mango-producing states. There are different varieties of mango in Nigeria depending on the region, locality, and tribe. They have been given nicknames such as 'Ogbomosho mango, Kerosene mango, and Peter mango' (Binta sugar/Jane mango) (Olotu et al., 2020).

Mango leaves, which are between 6-16 inches in length and lathery in texture are usually alternately arranged on the twigs. The young leaves are of pale green or pinkish color. In traditional medicine, extracts of mango leaves have been reported to have antimicrobial, antioxidant, anticancer, and anti-diabetic properties. Decoctions of mango leaves have also been used to treat fever, cough, diarrhea, hypertension,

asthma, colds, insomnia, and skin burns. It has also found use as a good herbal mouthwash (Muralikrishna et al., 2014). Similarly, Bharathi et al reported mango leaves to possess antipyretic, hypolipidemic, hepatoprotective, anticancer, gastroprotective, and anti-diabetic properties (Bharathi et al., 2017).

Mango leaves contain a significantly high amount of phenolic compounds. The chief being, mangiferin, often responsible for many of the pharmaceutical activities of this wonder plant (Kabir et al., 2017). From the ethnomedicinal point of view, this ability of various parts of mango is due to the presence of bioactive compounds such as flavonoids, saponins, glycosides, tannins, alkaloids, and anthocyanins.

From the foregoing literature search, it can be observed that several reports existed in the use of the *M. indica* leaf extracts for the synthesis of gold nanoparticles. However, reports on the anti-diabetic properties of the said gold nanoparticles are scanty. Hence, the present work.

MATERIALS AND METHODS

Reagents and Instrument

Some of the organic solvents required include methanol, ethanol and acetone. They were used for extraction. Polystyrene 96-well microtitre plates was used for anti-diabetic assay evaluation. Hydrochloric acid (HCl), sodium chloride, 2,4,6-tris(2-pyridyl)-s-triazine, sodium tetrachloroaurate (III) dihydrate, and iron (III) chloride hexahydrate. The following reagents are used: p-nitrophenyl-α-D-glucopyranoside (p-NPG), 3,5-dinitro salicylic acid (DNS), phosphate-buffered saline (PBS), glycine, alpha-glucosidase (Saccharomyces cerevisiae), alpha-amylase (procaine pancreas), sodium carbonate (Na_2CO_3), sodium dihydrogen phosphate, and disodium hydrogen phosphate. To track the distinctive peaks of the gold nanoparticles, a polar star Omega microtitre plate reader (BMG Labtech, Ortenberg, BW, Germany) was employed. The morphology of the Au NPs was investigated using a high-resolution transmission electron microscope (FEI Tecnai G2 F20 S-Twin HRTEM, running at 200 kV). For elemental analysis, a Zeiss Auriga Field Emission Scanning Electron Microscope equipped with an Oxford EDS system was utilized.

Collection and Preparation of samples

The leaves of *Mangifera indica* (Binta sugar mango) were collected from Science Secondary School B, Kangiwa of Bosso Local Government area, Minna, Niger State, Nigeria. 100.0 g of the sample collected was rinsed severally with tap water and then distilled water. The sample was dried at room temperature after which it was ground to powdered form. Then, 5.0g of the powdered sample materials was added to 100 ml of distilled water and heated to 90 ^oC for 10 min. The mixture was allowed to cool to room temperature and thereafter filtered using a Whatman filter paper. The filtrate - designated as leaf extract of *Mangifera indica* (LEMI)- is then ready for use as the reducing agent (Elbagory et al., 2016).

Preparation of gold salt solution

The method of Elbagory and colleagues was adopted. Briefly, some 2.0 g of $NaAuCl_4$ was added to 70 ml distilled water in a 100 ml volumetric flask and stirred thoroughly. Upon complete dissolution of the salt, more distilled water was added until the 100 ml mark. This gave a 1.0 mM solution of gold salt. (Elbagory et al., 2016).

Synthesis of gold nanoparticles

Gold nanoparticles was prepared through a simple green route. For every 250 ml of the filtrate (LEMI), 50 ml of the gold salt solution was added. The mixture was stirred at 30 rpm at the temperature of 90 ^oC for 30 min. Within this time; a ruby red coloration appeared to confirm the formation of gold nanoparticles (LEMI-AuNPs). This colloidal solution was allowed to stir continuously for further 1 hr at room temperature. Thereafter, the nanoparticles were centrifuged and washed severally to remove any unreacted substances. It was then dried in an oven at about 60 ^oC. The nanoparticles were then stored in a brown, air-tight container for subsequent use (Boruah et al., 2019).

Analysis of LEMI-AuNPs

A microplate reader was used to record the absorbance of the LEMI-AuNPs in the UV-visible region (BMG Labtech, Germany). Zetasizer (Malvern Instruments Limited, United Kingdom) was used to measure the size of the colloidal solution and the zeta potential at 25 and 90 degrees Celsius. The FEI Tecnai G2 20 field-emission gun, running in bright field mode at 200 kV, was used to take the TEM micrograph. Using the X-ray diffraction Model Broker AXS D8 advance at λkCuka1 = 1.5406 Å, the crystallinity of LEMI-AuNPs was verified. A Multiplate reader was used to take readings during the biological assay, which was carried out in a 96-well plate (Multiska Thermo Scientific, version 1.00.40).

Alpha-amylase Inhibitory Activities

This was accomplished by following the methodology of (Ponnanikajamideen & Rajeshkumar, 2019). To put it briefly, a 96-well plate was filled with LEMI, as well as LEMI-AuNPs, in serial concentrations of 100, 50, 25, 12.5, and 6.25µg/mL. After that, 20 µL of alpha-amylase (2U/mL) solution and 50 µL of phosphate buffer (100 mM, pH 6.9) were added. After 20 minutes of pre-incubation at 37 ^0C, 1% soluble standard was added, and the mixture was incubated for 30 minutes. After that, 100 µL of color reagent (DNS) was added, and the mixture was heated in a water bath for 10 minutes. Acarbose at different concentrations was used as the standard when measuring absorbance. In the absence of the exam, parallel solutions were set up as

$$Percentageinhibition = \left(1 - \frac{Q}{P}\right) * 100 \qquad (1)$$

where Q and P are the absorbances of the test samples and control respectively

Alpha-glucosidase Inhibitory Activities

With minor modifications, the methodology of Mahlo et al. (2024) was applied. In a 96-well plate, 20 µL of the LEMI or LEMI-AuNPs at different concentrations were combined with 50 µL of phosphate buffer, and the mixture was thoroughly mixed for 10 minutes at room temperature. After adding 50 µL of a 3 mM p-NPG as a substrate, the mixture was incubated at 37 ^oC for 20 minutes. The reaction was then finished by adding 50 µL of 0.1 M sodium carbonate. All other treatments were the same as in the alpha-amylase section, and the absorbance was measured at 405 nm.

RESULTS AND DISCUSSION

Spectroscopy of LEMI-AuNPs in the UV

The leaf extracts of several plant materials have been reported to house brilliant phytoconstituents which are responsible for the formation of nanoparticles. One of the easiest ways of confirming the successful synthesis is the use of UV Visible spectroscopy (Danazumi et al., 2024; Ihum et al., 2024). Here, a typical UV-visible spectra of LEMI-AuNPs with SPR at 539 nm is displayed in Figure 1. The effective production of gold nanoparticles is shown by the greatest absorption in this area. According to earlier research, the SPR for AuNPs typically ranges from 500 to 600 nm (Badeggi et al., 2020). Thus, LEMI-AuNPs' SPR is consistent with prior research.

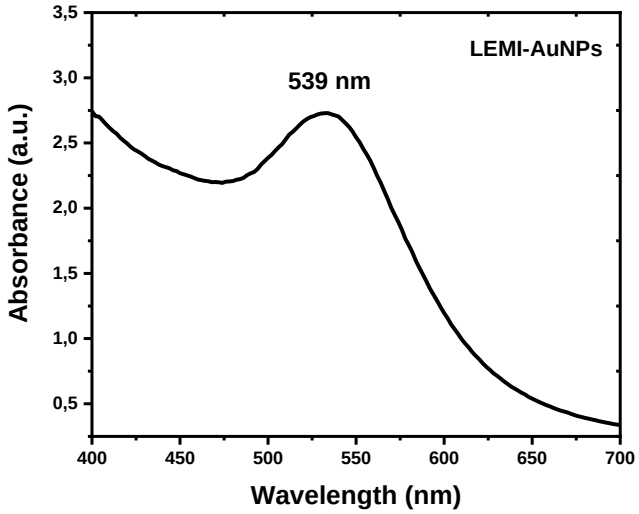

Figure 1: Ultra-violet Visible spectra of the LEMI-AuNPs

TEM, SAED and particle size distribution analysis of LEMI-AuNPs

The TEM analysis's micrographs demonstrate the formation of predominantly minuscule hexagonal AuNPs (Figure 2A). However, there are a few exceptions, where particles with different shapes, such as triangular and somewhat rectangular shaped particles were seen. The reduction and stabilization of the LEMI-AuNPs are facilitated by many phytoconstituents, including alkaloids, terpenoids, and flavonoids. Previous research has also demonstrated that particles of various shapes frequently arise from the production of plant extracts (Elbagory et al., 2017). The average size of LEMI-AuNPs, as determined from the micrograph in figure 2A, was 7.4 ± 0.9 nm. Smaller particles typically exhibit superior activities than larger ones. Additionally, there have been reports of using plant extracts with particles that are comparable in size (Badeggi et al., 2020). Similarly, TEM was used to characterize nanoparticles biosynthesized using *Cassia fistula* leaf extract and the authors found the particles in the range of 16-95 nm (Ihum et al., 2024). Therefore, prior research works provided strong support for our findings. The selected area electron diffraction (SAED), which was also acquired from the TEM device, is displayed in Figure 2B. The lattice fringes that give information about the crystallinity of LEMI-AuNPs are represented by the brilliant circular rings. As seen in the picture, the rings have been indexed to the 111, 200, 220, and 311 planes. Other investigations have shown that the XRD result is frequently complemented by the SEAD patterns(Kumar *& Kaur*, 2020).

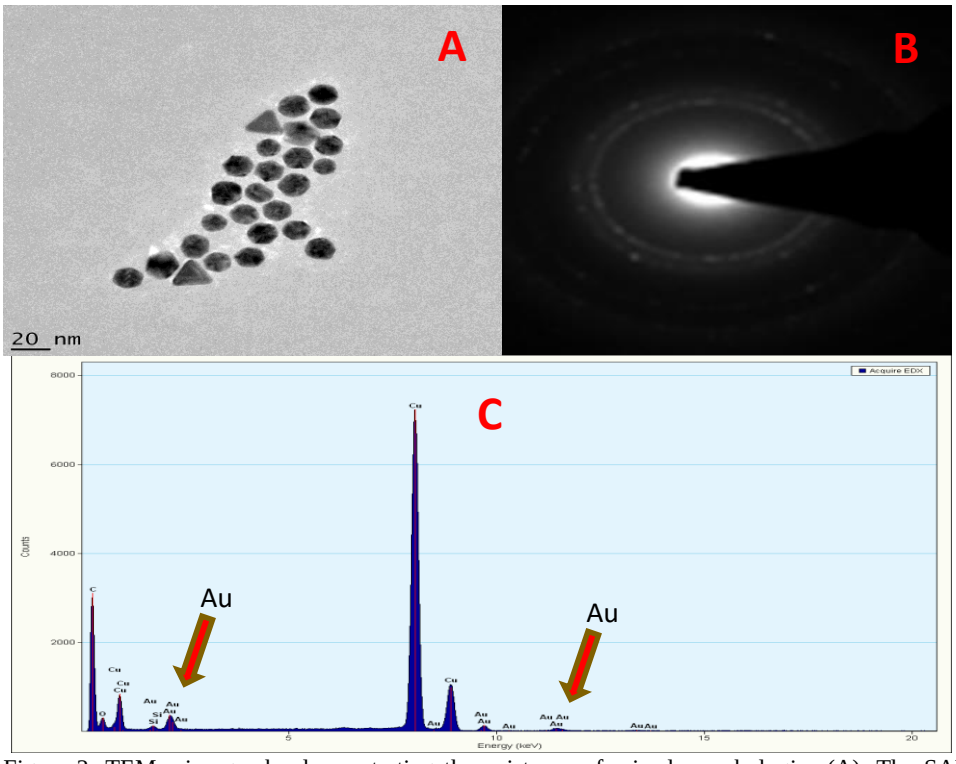

Figure 2: TEM micrographs demonstrating the existence of mixed morphologies (A). The SAED pattern (B) and particle size distribution (C) histograms of LEMI-AuNPs depicting presence of gold

Diffraction of X-rays Examination of LEMI-AuNPs

Figure 3 displays the X-ray diffraction (XRD) marking of LEMI-AuNPs. XRD analysis is commonly evaluated to understand the crystal nature of nanomaterials. For the LEMI-AuNPs, four distinct diffraction peaks were discernible in the two theta degrees of about 38, 44, 64, 78 and 83. These were associated with the 111, 200, 220, 311 and 222 planes of the face-centered cubic gold particles. A comparison with that of pure crystalline gold revealed that the LEMI-AuNPs are polycrystalline (file no. 04-0784). Similar findings were previously reported by Senthilkumar et al. (2019).

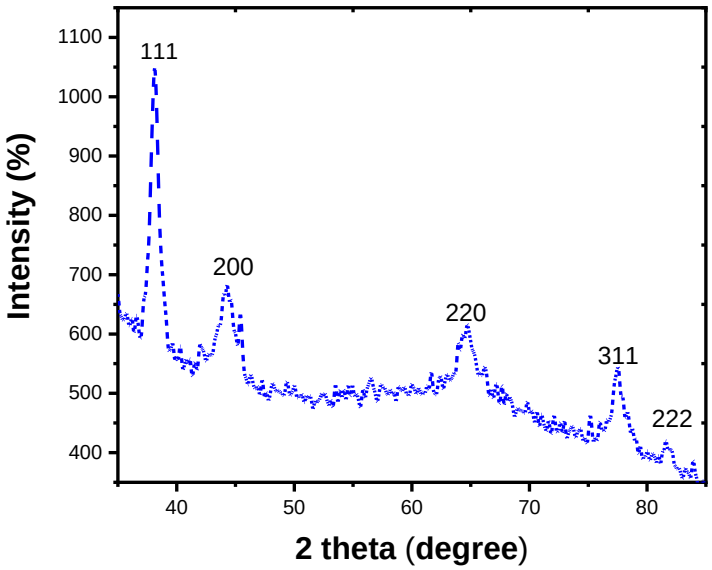

Figure 3: Showing XRD marking of the LEMI-AuNPs diffraction peaks

Dynamics of LEMI-AuNPs' Light Scattering (DLS)

After a successful synthesis of nanomaterials, the next most important thing is the examination of their shape, size and phase behavior. This must be done before any form of applications. Dynamic Light Scattering techniques are among other means of studying these (Badeggi et al., 2020). The Zetasizer, which was used to evaluate the DLS of the LEMI-AuNPs, supplied three essential pieces of information: the zeta potential (ZP), polydisperity index (PDI), and hydrodynamic size (HDS) of the colloidal solution. The average particle size in solution, as shown in Table 1, was found to be 31.74 nm, which is the HDS. This method allows for the rapid verification that as-synthesised nanoparticles are in the nanoscale region. Similar size of gold nanoparticles has been reported by Fang and colleagues (Fang et al., 2019). The degree of irregularity in the particle morphologies in the colloidal solution, on the other hand, is linked to the PDI. A unitless PDI is in the range of 0.01 to 0.7. The PDI score of 0.205 in this instance indicates that particles with comparable shapes prevail. In 2022, Badeggi and co-researchers reported PDI values of 0.170 and 0.467 for two silver nanoparticles they synthesized. These values fall within the standard recommended range and the later, close to the value obtained in the present work, further supporting our findings (Badeggi et al., 2022). The degree of stability of nanoparticles may vary depending on the kind and quantity of phytoconstituents acting as capping agents. The ZP values of the nanoparticles are frequently used to understand this. Without the use of external stabilizers, Table 1's ZP of -23.7 mV indicates moderate stability. Because stability is a crucial component, this result qualifies the LEMI-AuNPs for usage in biological systems. Similar previous researches involving gold nanoparticles recorded zeta potential values of -26.3 mV (Sadowski, 2010), and -2.9 to -90 mV (Pyell et al., 2015). Both positive and negative ZP values are possible. As a result, the negative value for LEMI-AuNPs verifies the anionic nature of the capping agents (Kumar & Kaur, 2020).

Table 1: Showing the values of HDS, PDI and ZP of LEMI-AuNPs

Sample	Hydrodynamic size (nm)	Polydisperity index	Zeta potential (mV)
LEMI-AuNPs	31.74	0.205	-23.7

Alpha-amylase and Alpha-glucosidase Inhibitory Activities

Alpha-amylase and alpha-glucosidase assays were used in this work to evaluate the antidiabetic effects of LEMI, LEMI-AuNPs and acarbose as the control (CTR). The same concentrations—100, 50, 25, 12.5 and 6.525 µg/mL—were used in both tests. The % inhibition for the LEMI, LEMI-AuNPs, and CTR for the two enzymes has been recorded in Table 2. From the table, LEMI demonstrated appreciable potential inhibition on the alpha-glucosidase more than the countertpart amylase. The correspounding gold nanoparticles showed better inhibiting abilities than the extract. This enhancement, which was even more pronounced against alpha-amylase may be due to increased surface area of the nanoparticles. Senthikumar and colleagues reported similar inhibition of alpha-glucosidase by gold nanoparticles synthesized from *Padina boergesenii* (Senthikumar et al., 2015). The nanoparticles synthesized using the extract of *Hypoxis hemerocallidea* by Mahlo et al showed antidiabetic activities close to our present work (Mahlo et al., 2024). These are confirming the agreement of our research work with previous studies.

Table 2: Inhibitory activities of LEMI and LEMI-Au NPs on alpha-glucosidase and alpha-amylase

Sample	Alpha-Glucosidase IC_{50} (µg/mL)	Alpha-Amylase IC_{50} (µg/mL)
LEMI	47.11 ± 0.4	59.51 ± 0.5
LEMI-Au NPs	35.31 ± 0.8	28.50 ± 0.3
Acarbose	24.20 ± 0.6	27.25 ± 0.6

*Acarbose: positive control.

CONCLUSION

Several spectroscopic and microscopic methods were used to comprehensively describe the greenly produced gold nanoparticles. For a while, it was discovered that the AuNPs were stable. They can therefore be used in biological applications. The enzymatic analysis showed strong suppression of alpha-amylase and alpha-glucosidase in comparison to the conventional medication, acarbose. In order to create gold nanoparticles with strong antidiabetic properties, the current study proposed a straightforward, easy, and eco-friendly method. For the in vivo analysis, more research is recommended.

ACKNOWLEDGEMENT

The authors wish to appreciate and thank TETFUND for the IBR intervention that funded this research. They also wish to thank IBB University for the opportunity and for providing the enabling environment.

REFERENCES

Ashraf, A., Zafar, S., Zahid, K., Salahuddin Shah, M., Al-Ghanim, K.A., Al-Misned, F. & Mahboob, S. 2019. Synthesis, characterization, and antibacterial potential of silver nanoparticles synthesized from Coriandrum sativum L. *Journal of Infection and Public Health*, **12(2):** 275–281. https://doi.org/10.1016/j.jiph.2018.11.002.

Badeggi, U.M., Ismail, E., Adeloye, A.O., Botha, S., Badmus, J.A., Marnewick, J.L., Cupido, C.N. & Hussein, A.A. 2020. Green Synthesis of Gold Nanoparticles Capped with Procyanidins from Leucosidea sericea as Potential Antidiabetic and Antioxidant Agents. *Biomolecules*, **10(3).**

Badeggi, U. M., Omoruyi, S. I., Ismail, E., Africa, C., Botha, S. & A. A. Hussein 2022. Characterization and Toxicity of Hypoxoside Capped Silver Nanoparticles. *Plants*, **11**, 1037

Bharathi, V., Firdous, J., Muhamad, N. & Mona, R. 2017. Green synthesis of Mangifera indica silver nanoparticles and its analysis using Fourier transform infrared and scanning electron microscopy. *National Journal of Physiology, Pharmacy and Pharmacology*, **7(12)**: 1364–1367.

Boruah, B.S., Daimari, N.K. & Biswas, R. 2019. Mangifera Indica Leaf Extract Mediated Gold Nanoparticles: A Novel Platform for Sensing of As(III). *IEEE Sensors Letters*, **3(3)**: 1.

Cho, N.H., Shaw, J.E., Karuranga, S., Huang, Y., da Rocha Fernandes, J.D., Ohlrogge, A.W. & Malanda, B. 2018. IDF Diabetes Atlas: Global estimates of diabetes prevalence for 2017 and projections for 2045. *Diabetes Research and Clinical Practice*, **138:** 271–281. https://doi.org/10.1016/j.diabres.2018.02.023.

Danazumi, K., Sani, A. M. Usman, A. K., & Umar, A. U. 2024. Synthesis of silver nanoparticles from *Lannea acida* via aqueous and methanolic leaf extract. *FUDMA Journal of Sciences,* **8(1),** 25-28.

Elbagory, A.M., Cupido, C.N., Meyer, M. & Hussein, A.A. 2016. Large scale screening of southern African plant extracts for the green synthesis of gold nanoparticles using microtitre-plate method. *Molecules*, **21(11).**

Fang, C.; Ma, Z.; Chen, L.; Li, H.; Jiang, C.; Zhang, W. 2019. Biosynthesis of gold nanoparticles, characterization and their loading with zonisamide as a novel drug delivery system for the treatment of acute spinal cordinjury. Journal of Photochemical and Photobiological B Biol., **190,** 72–75.

Ihum, T. A., Oledibe, C. F., Kurrah, A. I., Akande, E. J., Ajayi, O. A., Olatunji, J. T., Kayode, E. A., & Lawal, Z. O. 2024. Inhibitory activity of *Cassia fistula* synthesized selenium nanoparticles against moulds of groundnut. *FUDMA Journal of Sciences*, **8(3),** 242-248.

Kabir, Y., Shekhar, H.U. & Sidhu, J.S. 2017. Phytochemical Compounds in Functional Properties of Mangoes. *Handbook of Mango Fruit: Production, Postharvest Science, Processing Technology and Nutrition*, (June): 237–254.

Kumar, A. & Kaur, H. 2020. International Journal of Biological Macromolecules Sprayed in-situ synthesis of polyvinyl alcohol / chitosan loaded silver nanocomposite hydrogel for improved antibacterial effects. *International Journal of Biological Macromolecules*, **145:** 950–964. https://doi.org/10.1016/j.ijbiomac.2019.09.186.

Lee, Jaewook, Park, E.Y. & Lee, Jaebeom. 2014. Non-toxic nanoparticles from phytochemicals: Preparation and biomedical application. *Bioprocess and Biosystems Engineering*, **37(6):** 983–989.

Maddinedi, S. babu, Mandal, B.K. & Maddili, S.K. 2017. Biofabrication of size controllable silver nanoparticles – A green approach. *Journal of Photochemistry and Photobiology B: Biology*, **167**: 236–241. http://dx.doi.org/10.1016/j.jphotobiol.2017.01.003.

Mahlo, S. J., More, G. K., Oladipo, A. O. & Lebelo, S. L. 2024. In vitro α-amylase/α-glucosidase, cytotoxicity and radical scavenging potential of Hypoxis hemerocallidea synthesized magnesium oxide nanoparticles. *Discover Applied Sciences*, **6:62**.

Muralikrishna, T., Malothu, R., Pattanayak, M. & Nayak, P.L. 2014. Green Synthesis of Gold Nanoparticles using *Mangifera Indica* (Mango Leaves) Aqueous Extract. *World Journal of Nano Science & Technology*, **3(2)**: 66–73.

Olotu, P. & Author, C. 2020. Varieties of Mangifera indica L. (Anacardiaceae) used as food and medicine by the Idoma people of Eke-Ogodumu in Okpokwu local government Area of Benue State, Nigeria PN Olotu, IA Olotu, Gushit NM, Ejembi HO, Onche EU and Ajima U. *~ 6 ~ Journal of Pharmacognosy and Phytochemistry*, **9(5):** 6–10. www.phytojournal.com.

Ponnanikajamideen, M. & Rajeshkumar, S. 2019. In Vivo Type 2 Diabetes and Wound-Healing Effects of Antioxidant Gold Nanoparticles Synthesized Using the Insulin Plant Chamaecostus cuspidatus in Albino Rats. *Canadian Journal of Diabetes*, **43(2):** 82-89.e6. https://doi.org/10.1016/j.jcjd.2018.05.006.

Pyell, U., Jalil, A.H., Pfeiffer, C., Pelaz, B. & Parak, W.J. 2015. Characterization of gold nanoparticles with different hydrophilic coatings via capillary electrophoresis and Taylor dispersion analysis. Part I: Determination of the zeta potential employing a modified analytic approximation. *Journal of Colloid and Interface Science*, **450**: 288–300.

Renner, S., Blutke, A., Clauss, S., Deeg, C.A., Kemter, E., Merkus, D., Wanke, R. & Wolf, E. 2020. Porcine models for studying complications and organ crosstalk in diabetes mellitus. *Cell and Tissue Research*, **380(2):** 341–378.

Sadowski, Z. 2010. Biosynthesis and application of silver and gold nanoparticles, In: Perez D. P. (Ed), Silver Nanoparticles, InTech Publising, pp. 257–277.

Senthilkumar, P., Priya, L., Ranjith Santhosh Kumar, D.S., Bhuvaneshwari, J. and Prakash P. 2015. Potent α-glucosidase inhibitory activity of green synthesized gold nanoparticles from the brown seaweed *Padina boergesenii. International Journal of Recent Advances in Multidisciplinary Research*,**2(11)**, .0917-0923

Senthilkumar, P., Surendran, L., Sudhagar, B. & Ranjith Santhosh Kumar, D.S. 2019. Facile green synthesis of gold nanoparticles from marine algae Gelidiella acerosa and evaluation of its biological Potential. *SN Applied Sciences*, **1(4)**: 1–12. https://doi.org/10.1007/s42452-019-0284-z.